Environmental Health
Engineering and
Management Journal

Original Article

Environmental Health
Engineering and Management

CrossMark

The relationship between the characteristics of Biochar produced at different temperatures and its impact on the uptake of NO_3^--N

Maryam Ahmadvand[1*], Jaber Soltani[1*], Seyyed Ebrahim Hashemi Garmdareh[1], Maryam Varavipour[1]

[1]Department of Irrigation Engineering, Abouraihan Campus, University of Tehran, Iran

Abstract

Background: Nitrogen leaching from agricultural lands is a major threat to groundwater and surface waters. This study investigated the relationship between the characteristics of wheat-straw biochar produced at different temperatures and its impact on the uptake of NO3--N.

Methods: Three types of biochar were produced from wheat straw at three different pyrolysis temperatures of 300, 400 and 500°C, and sampling was done 3 times for each biochar. Physical and chemical characteristics of biochar were determined using a variety of methods including specific surface with methylene blue adsorption method, and elemental content with elemental analyzer, and water solubility with standard ASTM (D5029-28) method. Statistical analysis was performed using Freundlich and Langmuir models. Nitrate concentration was measured using a UV-V spectrophotometer with a wavelength of 500 nm.

Results: It was indicated that with an increase in biochar pyrolysis temperature from 300 to 500°C, the hydrogen, oxygen and nitrogen in the biochar were significantly decreased ($P < 0.05$) while the carbon content, surface area, density and water solubility in biochar ($P < 0.05$) were increased. The results also showed that the maximum nitrate adsorptive capacity of the three types of biochar occurred at pH=6 and contact time of 120 minutes. With increasing the temperature of biochar preparation, the efficiency of biochar nitrate adsorption increased significantly.

Conclusion: The present study shows that pyrolysis temperature greatly influences the biochar chemical and physical characteristics, and subsequently nitrate adsorption ability of the biochars. The wheat straw biochar, which is produced at a pyrolysis temperature of 500°C, has the highest adsorption capacity for nitrate.

Keywords: Biochar, Nitrates, Adsorption

Citation: Ahmadvand M, Soltani J, Hashemi Garmdareh SE, Varavipour M. The relationship between the characteristics of Biochar produced at different temperatures and its impact on the uptake of NO3--N. Environmental Health Engineering and Management Journal 2018; 5(2): 67–75. doi: 10.15171/EHEM.2018.10.

*Correspondence to:
Maryam Ahmadvand
Email: m_ahmadvand@ut.ac.ir;
Jaber Soltani
Email : jsoltani@ut.ac.ir

Introduction

Biochar as a beneficial substance can be used in agriculture and environment, and has attracted the attention of researchers. Biochar is a carbon-rich substance which is produced by the thermal decomposition of biomass under low oxygen or relatively low temperature, below 700°C (1). Biochar characteristics include a large specific surface area, a high density of negative surface charges, and characteristic pores and surface functional groups.

Nitrogen leaching from agricultural lands due to the increase in the use of nitrogen fertilizers is a major threat to groundwater and surface waters that leads to the occurrence of Eutrophication phenomenon (2). In recent studies, the ability of biochar in reducing nitrate

leaching and its impact on the nitrogen cycle in soil has been reported (3,4), so that by using biochar in soil (at 2.0 m depth), NH_4^+-N leaching reduced by 15%. Laird et al (5) reported a 11% reduction in nitrogen leaching in agricultural soils of the West Central America after adding biochar to the soil. The research showed that biochar has high potential in the adsorption of nitrogen and can be used as a soil amendment to reduce nitrogen losses. Even though, some studies indicated the low ability or inability of biochar to adsorb nitrogen. Hollister et al (6) did not observe any NO_3^--N adsorption by the biochar produced from corn and oak. Also, Yao et al (7) tested 11 types of biochar and found that only 2 types of biochar had the ability to adsorb nitrate. Gai at al (8) investigated the

physical and chemical properties of 12 biochars which were produced from wheat-straw, corn-straw and peanut-shell at pyrolysis temperatures of 400, 500, 600 and 700°C. They reported that biochar yield and contents of N, hydrogen and oxygen decreased as pyrolysis temperature increased from 400 to 700°C, whereas contents of ash, pH and carbon increased with higher pyrolysis temperatures. They also used the biochars for N sorption experiments. The results showed that none of the NO_3^-- N was adsorbed to biochars at different NO_3^- concentrations. Instead, some NO_3^-- N were even released from the biochar materials. They suggested further research is needed to investigate the application of biochars in reducing NO_3^-- N pollution. The inconsistency between the studies may be due to different characteristics of different biochars produced from various biomasses, as well as their different preparation conditions, and different initial concentration of nitrate or biochar mass. Therefore, it is essential to investigate the relationship between the characteristics of biochar and its impact on the uptake of NO_3^-- N.

Feedstock and temperature during pyrolysis are two factors that influence the molecular structure and pore-size distribution of biochar, and consequently affect the adsorption characteristics of biochar (1). In general, high pyrolysis temperature leads to larger specific surface area and higher aromaticity of biochar (9,10). Biochars produced from wheat residues at 500 to 700°C were well carbonized and their specific surface area were more than biochars which were produced at temperatures more than 300 to 400°C. Meanwhile, the results of Novak et al (11) show that biochar produced at low temperatures (250-400°C) in addition to having a stable aromatic structure, also have more C-H and C=O group factor that may be used as the positions of nutrients exchange after oxidation. Ahmad et al (12) reported that, by reducing the atomic ratio of H/C and O/C as a result of the removal of functional groups containing oxygen and hydrogen under the influence of temperature rise, biochars with low polarity and high aromatic properties can be produced. Kloss et al (13) investigated biochars of three feedstocks (wheat straw, poplar wood, and spruce wood) that were pyrolyzed at 400, 460, and 525°C. They found that lower pyrolysis temperatures resulted in the higher H/C ratios. As mentioned before, pyrolysis temperature and feedstock type are two factors that influence characteristics of biochar such as specific surface area, water solubility, and density which affect nitrate adsorption of biochar.

None of the previous studies on biochars have investigated the optimum biochar mass, pH and contact time.

Therefore, the aim of this study was to investigate the relationship between wheat-straw biochar pyrolysis temperature and physical and chemical characteristics of the produced biochar, the effects of pyrolysis temperature on nitrate absorption of biochar, the effects of initial concentration of nitrate solution on nitrate absorption and also to determine the optimum biochar mass, pH and contact time. In order to perform the required experiments, wheat-straw biochars were produced at 300, 400, and 500°C.

Methods

The biochar used in this study was prepared from wheat straw. For this purpose, the wheat straws were cut into 2 cm pieces and then were placed in the oven for 2 hours at 70°C. After washing the straws with distilled water and passing them through the sieve No. 18, the straws were put in an electric furnace without oxygen at 300, 400 and 500°C for 90 minutes in order to produce biochar (10). The biochar production rate at each temperature was calculated as Equation 1 (8):

$$R\ (\%) = (M_B/M_F) \times 100 \qquad (1)$$

In this regard, R is biochar production rate, M_B, the mass of biochar and M_F, the mass of Feedstock. The chemical and physical characteristics of biochars are listed in Tables 1 and 2. Elemental contents of C (carbon), hydrogen (H), nitrogen (N) and oxygen (O) were determined using an elemental analyzer (Euro Vector S.P.A- Euro EA 3000). Table 1 shows the results of analysis of CHNO using the elemental analyzer.

To determine the specific surface area of biochar, methylene blue adsorption method was used. For this purpose, different concentrations (1, 5, 10, 15, and 20 mg/L) of methylene blue were prepared in order to prepare the calibration graph and their concentrations were measured and recorded by the UV-Vis spectrophotometer (Hach, DR5000) with a wavelength of 600 nm. Then, 0.1 g biochar was poured in 100 mL methylene blue solution with concentration of 17.46 mg/L and was shaken in a thermostatic shaker (VDRL-TM52) at 150 rpm for 1 hour. After separating the adsorbent from the solution by filter paper, the final concentration was measured and biochar specific surface was calculated by Equation 2 (14):

$$s_g = b \frac{N_A}{M_{MB}} \sigma_{MB} \quad (2)$$

In this equation, b is adsorption capacity derived from the uptake curve (mg/mg), N_A, Avogadro's number of

Table 1. The amount of chemical composition and atomic ratio of biochars produced at different temperatures

Biochar	Produced Biochar (%)	C	N	H	O	C/N	O/C	H/C
W-BC300	34.1	55.2	1.7	3.8	24.85	38.6	0.34	0.83
W-BC 400	29.2	58.3	1.4	3.1	20.36	50.0	0.26	0.64
W-BC 500	26.3	70.1	1.3	2.6	16.14	64.4	0.17	0.44

6.02×10^{23}, M_{MB}, methylene blue molecular weight equal to 319.85 g/mol, σ_{MB}, the area occupied by a methylene blue molecule of 1.08 nm^2 and s_g, adsorbent surface area in m^2/g. In this study, water solubility of biochar was measured using standard ASTM (American Society for Testing and Materials) (D5029-98) [15]. For this purpose, 5 g biochar combined with 50 mL of boiled water was boiled for 15 minutes.

Then, the solution was passed through filter paper and 10 mL of the filtrated sample was poured into a clean container which was weighed previously; then the container was placed in the oven at 150°C for 1 hour so that the sample solution evaporated and the remaining sample solution was completely dried. After drying, the remainder and its container were carefully weighed; then, the water solubility of each adsorbent was determined according to the Equation 3.

$$Water\ Solublility\ (\%) = \frac{(B-A) \times (D)}{(C) \times (E)} \tag{3}$$

In this equation, A is the initial weight of the container, B, the weight of container along with dry weight, D, consumed boiled water (mL), C, the volume of biochar (g), and E, the volume of filtered samples (mL). To determine the density of studied biochar, a certain volume of biochar was weighed and then the samples were dried in the oven at 105°C for 24 hours. After drying, the dried samples were weighed again. The weight of samples after drying was considered as dry weight. Finally, the density of adsorbents was determined using Equation 4 [16].

$$\rho = \frac{M_s}{V_t} \tag{4}$$

In this equation, M_s is the dry weight (g), V_t, total volume of the sample (mL) and ρ, the density of adsorbent. In order to evaluate the amount of nitrate surface adsorption by biochar prepared from wheat straw at temperatures of 300, 400 and 500°C, batch test was performed and exposure time was calculated by changing various parameters including pH, adsorbent and nitrate concentration. Stock solution (1000 mg/L) was prepared using sodium nitrate salt. Then, solutions with different concentrations (10, 20, 40, 80, 160 and 320 mg/L) of the main stock solution were prepared. In all tests, the volume of the solutions used was 50 mL and pH values of the solutions was regulated by NaOH and HCL of 0.1M. In order to determine the effect of pH on nitrate uptake by biochar, ten 200 mL beakers were washed with distilled water and 3.0 M nitric acid solutions, and 1 g of adsorbent was poured into each of the beakers. Then, 50 mL of the solution with a concentration of 20 mg/L was added to each of the beakers and pH of the solution was formulated in various amounts of 3 to 12. pH of the solution was measured using a pH meter (Metrohm 712 Conductometer). The solution was kept at room temperature and shaken in a thermostatic shaker at 150 rpm for 24 hours. Afterwards, adsorbent was separated from the solution using filter paper and nitrate concentration was measured using a UV-Vis spectrophotometer (model Hach, DR5000) with a wavelength of 500 nm. Then, the capacity and efficiency of adsorption were determined through Equations 5 and 6, respectively [17].

$$q_e = \frac{c_0 - c_e}{m} \times v \tag{5}$$

$$R = \frac{c_0 - c_e}{c_0} \times 100 \tag{6}$$

C_0 (mg/L) represents the initial nitrate concentration in the solution, C_e (mg/L), nitrate concentrations in the solution at equilibrium (mg/L), m, biochar mass (g), v, volume of the solution (L), q_e, adsorption capacity (mg/g) and R, adsorption percentage. To determine the optimal adsorbents dosage, different volumes (0.1, 0.2, 0.3, 0.4, 0.5, 0.6 0.7, 0.8, 0.9, and 1 g) of the studied adsorbent was added to 50 ml solution at a concentration of 20 mg/L. pH of the solution was regulated on the optimal setting, then the solution was shaken in a thermostatic shaker at 150 rpm for 120 minutes. Adsorbent was separated from the solution using filter paper and concentration of the solution was determined. Then, the efficiency and amount of the adsorption were determined [17].

To determine the effect of the initial concentration, the efficiency of adsorption of various concentrations (10, 20, 40, 80, 160 and 320 mg/L) at the optimum condition obtained from previous stages (pH optimum, equblirium time and optimum adsorbent mass) was tested. To test the adsorption isotherm, 0.4 g of the adsorbent was added to 50 mL of the solution with different concentrations (10, 20, 40, 80, 160 and 320 mg/L) and shaken in a thermostatic shaker at 150 rpm for a certain time (equilibrium time obtained from adsorption kinetics). Finally, adsorbent was separated from the solution through filter paper.

Adsorption isotherms

The nitrate adsorption data were fitted to linear Freundlich and Langmuir models. Langmuir adsorption isotherm indicates one monolayer adsorption on the homogeneous surface without any reaction between the adsorbed molecules and homogeneous adsorbed energy on the surface by Equation 7 [17].

$$q_e = \frac{q_e b\ c_e}{k_l + k_l c_e} \tag{7}$$

In this equation, c_e is the concentration of adsorbed material at equilibrium in the liquid phase (mg/L), q_e, the amount of adsorbed ions per unit mass of the adsorbent at equilibrium (mg/L), b, the capacity of adsorption in the solid phase (mg/L) and k_l, constant adsorption [18]. Freundlich adsorption isotherm is an empirical model used to explain the multi-layer adsorption with heterogeneous distribution of energy by the reaction

between the concentration of adsorbed material in the equilibrium molecules. Equation 8 shows the isotherms.

$$q_e = k_f c_e^{\frac{1}{n}} \tag{8}$$

In this equation, k_f is constant isotherm in relation to the adsorption (L/g) and 1/n is the density of adsorption which varies with the non-uniformity of materials (19). One of the most important studies in the process of adsorption is the effect of contact time with the adsorption amount; which is known as kinetics studies. To study the mechanisms controlling the adsorption process, kinetic models of Lagergren's pseudo-first-order and Hu's pseudo-second-order are used . Equation 9 shows Lagergren model:

Log(q_e-q_t)=logq_e- (k_lt/2.303) (9)

In this equation, q_e and q_t respectively indicate the amount of ions adsorbed (mg/g) at equiblirium time and t time, and k_l is constant absorbed in the Lagergren model. k_l values are calculated through plotting of log (q_e - q_t) versus t (20). Hu model indicate it in linear model as Equation 10:

$$\frac{t}{q_t} = \frac{1}{k_2 q_e^2} + \frac{t}{q_e} \tag{10}$$

In this equation, k_2 is the adsorption constant rate (g/mg. min) (21). To obtain the coefficients of Hu model, $\frac{t}{q_t}$, is plotted verses t. Through plotting this curve, a straight line with a slope of $\frac{1}{q_e}$ and intercept of $\frac{1}{k_2 q_e^2}$ is obtained, through which, the constants can be calculated (20).

Statistical analysis

Standard deviations, means, RMSE (Root Mean Square Error) and R^2 were used to express the results. The RMSE is a frequently used measure of the difference between values predicted by a model and the values actually observed from the environment that is being modelled. The RMSE of a model prediction with respect to the estimated variable X_{model} is defined as the square root of the mean squared error. Equation 11 shows RMSE:

$$RMSE = \sqrt{\frac{\sum_{i=1}^{n}(X_{obs;i} - X_{modele;i})^2}{n}} \tag{11}$$

where X_{obs} is observed values and X_{model} is modelled values at time/place I (22).

To plot the figures and to perform statistical analysis, Origin 8.1 and SAS 9.1, respectively, were used. Duncan's multiple range test was used to test significant differences and Pearson test (two-tailed test) was used to analyze the correlation. Statistically significant values were considered at $P < 0.05$.

Sampling was done 3 times from biochars produced from wheat straw at 3 different pyrolysis temperatures of 300, 400 and 500°C. Analysis of the samples was expressed as the average of three replicates.

Results

The biochar production rate and element contents of biochar from wheat straw at 3 different pyrolysis temperatures of 300, 400 and 500°C are given in Table 1. As shown in Table 1, with an increase in the pyrolysis temperature of biochar from 300 to 500°C, biochar production rate decreased from 34.1% to 26.3%. Content of C, which is the major constituent of the biochars, significantly increased with higher pyrolysis temperatures ($P < 0.05$), however, contents of N, H and O decreased by approximately 76% , 68% and 65%, respectively, as pyrolysis temperature increased from 300°C to 500°C (Table 1). Table 1 shows that with an increase in the pyrolysis temperature of biochar from 300°C to 500°C, the atomic C/N ratio was significantly increased from 38.6% to 64.4 % ($P < 0.05$), however, the atomic O/C and H/C ratios were decreased from 0.34% and 0.83% to 0.17% and 0.44%, respectively.

Table 2 illustrates density, water solubility and specific surface area of biochars produced at different temperatures. It shows that with an increase in biochar pyrolysis temperature from 300 to 500°C, specific surface area was significantly increased from 49.8 to 64.8 (cm²/g) ($P < 0.05$). Also, biochar solubility in water and density was significantly increased with higher pyrolysis temperatures ($P < 0.05$).

Figure 1 indicates the effect of pH on nitrate adsorption efficiency of biochars prepared at different temperatures (300, 400 and 500°C). As shown in this figure, in all three types of biochar, with an increase in the pH of the solution from 3 to 12, the adsorption efficiency of nitrate was increased significantly in all three types of biochar ($P < 0.05$). The maximum adsorption efficiency of nitrate was observed at pH = 6. With an increase in pH, the adsorption efficiency was decreased and its minimum value was observed at pH = 12.

The effect of biochar mass on nitrate adsorption efficiency of biochars which were prepared at three different temperatures, are presented in Figure 2. As shown in this figure, with an increase in the volume of biochar from 1.0 to 4.0 g, the nitrate adsorption efficiency in W-BC 300, W-BC 400 and W-BC 500 was significantly increased from 4.5%, 6% and 9% to 19%, 24.5% and 29%, respectively

Density, water solubility and specific surface of biochars produced at different temperatures

Biochar	Specific Surface Area (cm²/g)	Solubility in Water (%)	Density (g/cm³)
W-BC 300	49.8	31.2	**0.10**
W-BC 400	59.9	32	**0.13**
W-BC 500	64.8	34.8	**0.14**
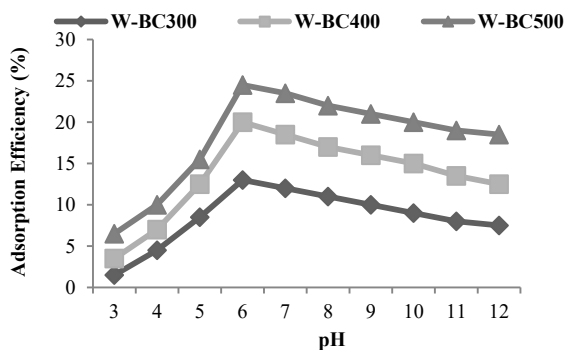
Figure 1. The changes of nitrate adsorption efficiency by biochar to pH.

Figure 3. Nitrate adsorption efficiency by biochars produced at different temperatures to time.

Figure 2. The mass effect of biochars produced at different temperatures on nitrate uptake.

Figure 4. The effect of initial concentration on nitrate adsorption efficiency by biochars produced at different temperatures.

($P<0.05$). However, by increasing biochar volumes from 0.4 to 1 g, the adsorption efficiency remained fairly stable. Thus, 4.0 g biochar was selected as the biochar optimal mass for the nitrate uptake.

After determining biochar mass and optimal pH, the effect of equilibrium time on nitrate uptake by biochars were investigated. At this stage, 4.0 g biochar (optimal mass) was added to nitrate solution with a concentration of 20 mg/L (optimum concentration). pH was considered equal to 6 and the contact time was changed from 10 to 240 minutes.

Figure 3 shows the changes in nitrate adsorption efficiency in various biochars along with time changes. As shown in this figure, by increasing the contact time, the nitrate adsorption efficiency in all three types of biochars was increased significantly ($P<0.05$) and reached its maximum value at 120 minutes. After this time, the changes in the efficiency of adsorption were not significant ($P<0.05$).

Figure 4 indicates the effect of initial concentration of nitrate on nitrate adsorption efficiency of biochars prepared at different temperatures (300, 400 and 500°C). As shown in this figure, by increasing the initial nitrate concentration from 10 to 320 ppm, the nitrate adsorption efficiency was reduced in W-BC 300, W-BC 400 and W-BC 500 from 23%, 30% and 37% to 6.3%, 9.7% and 11.3%, respectively.

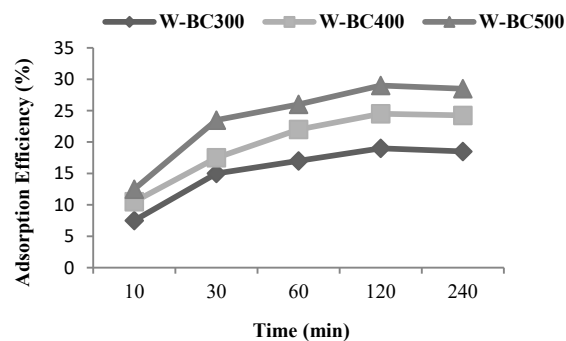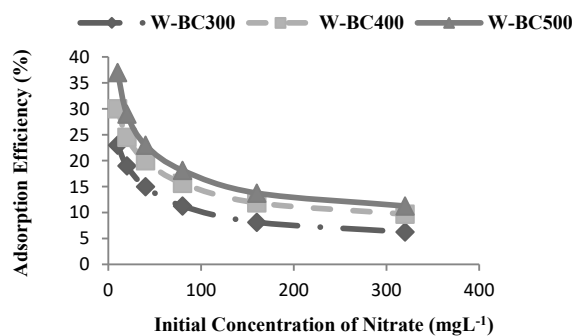The effect of initial concentration of nitrate on adsorption

capacity of biochars produced at different temperatures are presented in Figure 5. The results show that with an increase in the initial concentration of nitrate, the adsorption capacity of all 3 types of biochar was significantly increased ($P<0.05$).

Figures 6-8 respectively indicate the fitting results of kinetics models of nitrate uptake by biochars produced at 300, 400 and 500°C at pH = 6. The fitting results of models are presented in Table 3.

Figures 9-11 respectively indicate the results of fitting isotherm models with experimental data of nitrate uptake by biochar produced at 300, 400 and 500°C at pH = 6. The Freundlich and Langmuir isotherm constants and
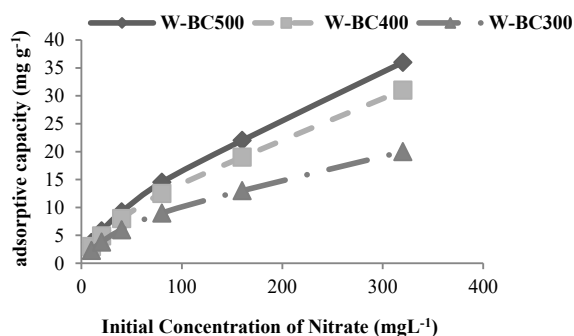

Figure 5. The effect of initial concentration of nitrate adsorption capacity by biochar produced at different temperatures.
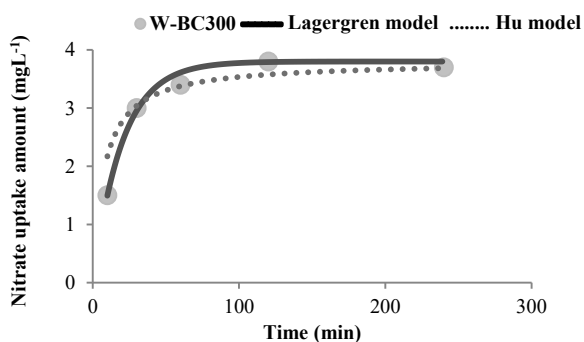
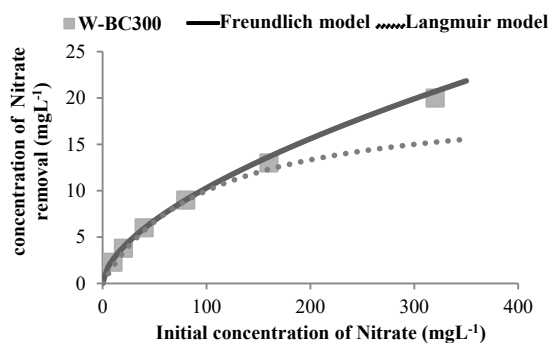**Figure 6**. Fitting results of kinetics models of nitrate uptake by biochar produced at 300°C.

Figure 9. Fitting results of isotherm models on experimental data of nitrate uptake by biochar produced at 300°C.
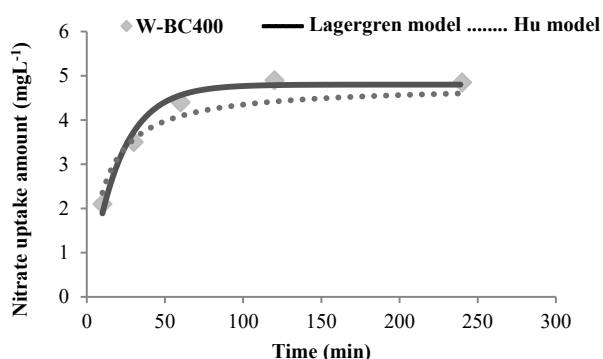

Figure 7. Fitting results of kinetics models of nitrate uptake by biochar produced at 400°C.
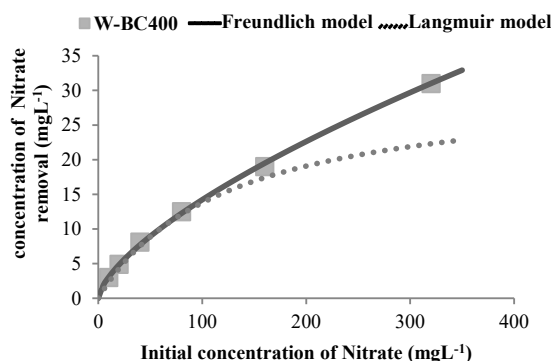

Figure 10. Fitting results of isotherm models on experimental data of nitrate uptake by biochar produced at 400°C.
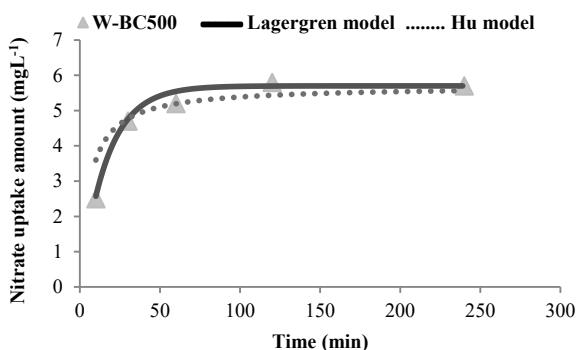

Figure 8. Fitting results of kinetics models of nitrate uptake by biochar produced at 500°C.
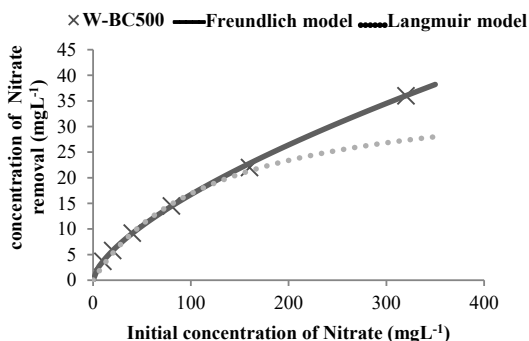

Figure 11. Fitting results of isotherm models on experimental data of nitrate uptake by biochar produced at 500°C.

nitrate adsorption correlation coefficients for different biochars are presented in Table 4. Adsorption of nitrate with different biochars was better fitted to Freundlich isotherm model, with higher R^2 values than that of Langmuir model. Although both K_F and n in Freundlich model affect nitrate adsorption isotherms, but it seems that K_F plays a main role in reflecting differences of nitrate adsorption ability between biochars derived from different feedstocks. W-BC500 with a greater K_F value in the isotherm had a relatively high nitrate adsorption

Table 3. Fitting results of kinetics models of nitrate uptake by biochar produced at different temperatures

Biochar	Lagergren Model				Hu Model			
	RMSE	R^2	q_e	K_1	RMSE	R^2	q_e	K_2
W-BC300	0.137	0.98	3.8	0.05	0.707	0.91	3.8	**0.035**
W-BC400	0.21	0.97	4.8	0.05	0.389	0.89	0.338	**0.02**
W-BC500	0.214	0.95	5.7	0.06	0.74	0.87	5.7	**0.03**

Table 4. Fitting results of isotherm models on experimental data of nitrate uptake by biochar

Biochar	Freundlich Model				Langmuir Model			
	RMSE	R^2	1/n	K_f	RMSE	R^2	Q_{max}	K_1
W-BC300	1.013	0.97	0.6	0.65	4.86	0.73	20	**0.01**
W-BC400	0.315	0.95	0.67	0.65	4.353	0.7	31	**0.008**
W-BC500	0.46	0.97	0.66	0.8	5.06	0.81	38	**0.008**

ability compared with W-BC400 and W-BC300.

Discussion

Table 1 shows that biochar production rate significantly increased with higher pyrolysis temperature (P<0.05). The reason is that at high temperatures, the loss of volatile materials is more. The results are consistent with the results obtained by Novak et al (11) and Gai et al (8). However, Khanmohammadi et al (23) showed that with an increase in the pyrolysis temperature of biochar from 300 to 700°C, biochar production decreased from 72.5% to 52.9%.

As shown in Table 1, biochar carbon content, which is the main component of the biochar, increased with the increase in biochar pyrolysis temperature. This was due to the increased carbonization at high temperatures with a high degree of C in aromatic structures (12). Ahmad et al (12) and Gai et al (8) obtained similar results in this regard, however, Khanmohammadi et al (23) showed that biochar produced at low temperatures had higher total organic carbon content. The results shows that with an increase in biochar pyrolysis temperature from 300 to 500°C, the content of H and O reduced to 68% and 65%, respectively. Gai et al (8) showed that content of H and O decreased by approximately 60% and 30%, respectively, as pyrolysis temperature increased from 400˚C to 700˚C (13). This can be due to the removal of water, hydrocarbons, tarry vapors, carbon monoxide and carbon dioxide during the carbonization process (24), also some of the contents of carbon and hydrogen were categorized as organic functional groups (10). All the obtained biochars have a little nitrogen (1.3 to 1.7%). Similar results were also obtained by other researchers in this regard (8,24). As it can be seen in Table 1, the atomic ratios of elements, which estimate the aromaticity (H/C) and polarity (O/C) of biochar, were significantly influenced by pyrolysis temperature of biochar. Chun et al (10) and Chen et al (25) found similar results in this regard and reported that at higher ratio of H/C, the level of carbonization and aromatic of biochar is less. Also, the ratio of O/C at high temperatures decreased, which indicates an decrease in the hydrophilic property of biochar surface at high temperatures.

As shown in Table 2, specific surface area was significantly affected by the pyrolysis temperature. Ding et al (4), Gai et al (8) and Mimmo et al (26) found similar results in this regard. This is likely due to the loss of H- and O-carrying functional groups, including aliphatic alkyl-CH_2 , ester C=O, aromatic -CO and phenolic OH groups, in biochars produced at high temperatures, which greatly enlarged their surface areas (25,26).

Regarding Figure 1, the reason for nitrate adsorption behaviour is that in low pH levels, biochar has a positive charge that causes biochar to be more likely to attract the negative charged nitrate. At pHs more than 6, OH ions will compete with nitrate ions for adsorption at biochar surface and decrease the nitrate uptake capacity by occupying adsorptive spaces (27). Also, at high pH levels, negative charge increases at adsorbent surface which subsequently reduces the nitrate absorption efficiency. The results obtained in this research are consistent with the findings of previous studies (27-29)

As shown in Figure 1, by increasing the biochar preparation temperature, nitrate adsorption efficiency also increased, which is consistent with the findings of Chun et al (10) and Gai et al (8). The reason is that with an increase in the temperature of biochar preparation, specific surface area and porosity increases and consequently increases the amount of nitrate uptake.

In this study, 4.0 g biochar was selected as the biochar optimal mass for nitrate uptake. Because with an increase in the amount of biochar from 1.0 to 4.0 g, the nitrate absorption efficiency significantly increases (P<0.05), which is likely to be due to the increase in the especial surface area and adsorbent spaces. However, by increasing biochar from 0.4 to 1 g, the adsorption efficiency remained fairly stable. To explain these observations, it can be said that biochars due to their high specific surface in the concentration more than 0.4 g, react and attract each other and their ability to adsorb is reduced. Surprisingly, no study has been determined the optimal mass of biochar in this way. But similar studies have been conducted to determine the optimal mass of other adsorbents, which have reported similar results (27).

According to the results of this study, equiblirium time for nitrate uptake was 120 m. In this period of time, solid and liquid phases reached to a balanced state and the rate of nitrate uptake to the surface of biochar and releasing rate of ions from the surface of the adsorbent particles into the solution were equal, which is consistent with the results of study by Farasati et al (27).

To explain the cause of observations in Figure 4, it can be said that in high concentrations, the adsorption efficiency decreases due to the saturation of adsorption situations.

As shown in Figure 5, by increasing the initial nitrate concentration, adsorption capacity increasesd, which

is probably due to the increased driving force in high concentrations. But this fills all the adsorption places quickly and thus the total nitrate adsorption reduces (30). Also Figure 4 shows that with increasing the biochar preparation temperature, the nitrate adsorption efficiency of biochar increased.

According to the results presented in Table 3 and Figure 6, it is concluded that in W-BC 300, W-BC 400 and W-BC500, Lagergren model with coefficient of 98.0, 97.0 and 95.0 and root-mean-square error (RMSE) of 0.044, 0.127 and 0.126 (R^2 more and RMSE less), respectively, is more successful than the Hu model.

Table 4 and Figure 7 indicate the fitting results of isotherm models on experimental data of nitrate uptake by biochar. The comparison of R^2 and RMSE in Freundlich and Langmuir models shows that nitrate adsorption process in all three types of biochar obeys the Freundlich model.

Conclusion

The results of the present study indicate that pyrolysis temperature greatly influences the biochar chemical and physical characteristics, which further influences nitrate adsorption ability of the biochars. The wheat straw biochar which produced at a pyrolysis temperature of 500˚C had the largest adsorption capacity for nitrate.

Acknowledgments

Ethical issues

The authors hereby certify that all data collected during the study is as stated in the manuscript, and no data from the study has been or will be published elsewhere separately.

Competing interests

The authors declare that thay have no competing interests.

Authors' contributions

MA contributed to the suggestion of problem. JS contributed to design of experiment, data collection and writing down this paper. SEHG contributed to physical experiments & MV contributed to chemical experiments. All authors contributed in article approval.

References

1. Keiluweit M, Nico PS, Johnson MG, Kleber M. Dynamic molecular structure of plant biomass-derived black carbon (biochar). Environ Sci Technol 2010; 44(4): 1247-53. doi: 10.1021/es9031419.

2. Zhu A, Zhang J, Zhao B, Cheng Z, Li L. Water balance and nitrate leaching losses under intensive crop production with Ochric Aquic Cambosols in North China Plain. Environ Int 2005; 31(6): 904-12. doi: 10.1016/j.envint.2005.05.038.

3. Galvez A, Sinicco T, Cayuela ML, Mingorance MD, Fornasier F, Mondini C. Short term effects of bioenergy by-products on soil C and N dynamics, nutrient availability and biochemical properties. Agric Ecosyst Environ 2012; 160: 3-14. doi: 10.1016/j.agee.2011.06.015.

4. Ding Y, Liu YX, Wu WX, Shi DZ, Yang M, Zhong ZK. Evaluation of biochar effects on nitrogen retention and leaching in multi-layered soil columns. Water Air Soil Pollut 2010; 213(1): 47-55. doi: 10.1007/s11270-010-0366-4.

5. Laird D, Fleming P, Wang B, Horton R, Karlen D. Biochar impact on nutrient leaching from a Midwestern agricultural soil. Geoderma 2010; 158(3-4): 436-42. doi: 10.1016/j.geoderma.2010.05.012.

6. Hollister CC, Bisogni JJ, Lehmann J. Ammonium, nitrate, and phosphate sorption to and solute leaching from biochars prepared from Corn Stover (L.) and Oak wood (spp.). J Environ Qual 2013; 42(1): 137-44. doi: 10.2134/jeq2012.0033.

7. Yao Y, Gao B, Zhang M, Inyang M, Zimmerman AR. Effect of biochar amendment on sorption and leaching of nitrate, ammonium, and phosphate in a sandy soil. Chemosphere 2012; 89(11): 1467-71. doi: 10.1016/j.chemosphere.2012.06.002.

8. Gai X, Wang H, Liu J, Zhai L, Liu S, Ren T, et al. Effects of feedstock and pyrolysis temperature on biochar adsorption of ammonium and nitrate. PLoS One 2014; 9(12): e113888. doi: 10.1371/journal.pone.0113888.

9. Ahmad M, Lee SS, Dou X, Mohan D, Sung JK, Yang JE, et al. Effects of pyrolysis temperature on soybean stover- and peanut shell-derived biochar properties and TCE adsorption in water. Bioresour Technol 2012; 118: 536-44. doi: 10.1016/j.biortech.2012.05.042.

10. Chun Y, Sheng G, Chiou CT, Xing B. Compositions and sorptive properties of crop residue-derived chars. Environ Sci Technol 2004; 38(17): 4649-55.

11. Novak JM, Lima I, Xing B, Gaskin JW, Steiner C, Das KC, et al. Characterization of designer biochar produced at different temperatures and their effects on a loamy sand. Ann Environ Sci 2009; 3: 195-206.

12. Ahmad M, Lee SS, Rajapaksha AU, Vithanage M, Zhang M, Cho JS, et al. Trichloroethylene adsorption by pine needle biochars produced at various pyrolysis temperatures. Bioresour Technol 2013; 143: 615-22. doi: 10.1016/j.biortech.2013.06.033.

13. Kloss S, Zehetner F, Dellantonio A, Hamid R, Ottner F, Liedtke V, et al. Characterization of slow pyrolysis biochars: effects of feedstocks and pyrolysis temperature on biochar properties. J Environ Qual 2012; 41(4): 990-1000. doi: 10.2134/jeq2011.0070.

14. Bestani B, Benderdouche N, Benstaali B, Belhakem M, Addou A. Methylene blue and iodine adsorption onto an activated desert plant. Bioresour Technol 2008; 99(17): 8441-4. doi: 10.1016/j.biortech.2008.02.053.

15. American Society for Testing and Materials. Standard test method for water solubles in activated carbon. ASTM; 2014.

16. Miller RW, Donahue RL. Soils: An introduction to Soils and Plant Growth. 6th ed. Englewood Cliffs, New Jersey: Prentice-Hall Inc; 1990. p. 60.

17. Bhatnagar A, Kumar E, Sillanpaa M. Nitrate removal from water by nano-alumina: Characterization and sorption

studies. Chem Eng J 2010; 163(3): 317-23. doi: 10.1016/j.cej.2010.08.008.

18. Li L, Liu F, Jing X, Ling P, Li A. Displacement mechanism of binary competitive adsorption for aqueous divalent metal ions onto a novel IDA-chelating resin: isotherm and kinetic modeling. Water Res 2011; 45(3): 1177-88. doi: 10.1016/j.watres.2010.11.009.

19. Escudero C, Poch J, Villaescusa I. Modelling of breakthrough curves of single and binary mixtures of Cu(II), Cd(II), Ni(II) and Pb(II) sorption onto grape stalks waste. Chem Eng J 2013; 217: 129-38. doi: 10.1016/j.cej.2012.11.096.

20. Malekian R, Abedi-Koupai J, Eslamian S, Mousavi SF, Abbaspour KC, Afyuni M. Ion-exchange process for ammonium removal and release using natural Iranian zeolite. Appl Clay Sci 2011; 51(3): 323-9. doi: 10.1016/j.clay.2010.12.020.

21. Olgun A, Atar N, Wang S. Batch and column studies of phosphate and nitrate adsorption on waste solids containing boron impurity. Chem Eng J 2013; 222: 108-19. doi: 10.1016/j.cej.2013.02.029.

22. Chai T, Draxler RR. Root mean square error (RMSE) or mean absolute error (MAE)? – Arguments against avoiding RMSE in the literature. Geosci Model Dev 2014; 7(3): 1247-50. doi: 10.5194/gmd-7-1247-2014.

23. Khanmohammadi Z, Afyuni M, Mosaddeghi MR. Effect of pyrolysis temperature on chemical and physical properties of sewage sludge biochar. Waste Manag Res 2015; 33(3): 275-83. doi: 10.1177/0734242x14565210.

24. Ok YS, Yang JE, Zhang YS, Kim SJ, Chung DY. Heavy metal adsorption by a formulated zeolite-Portland cement mixture. J Hazard Mater 2007; 147(1-2): 91-6. doi: 10.1016/j.jhazmat.2006.12.046.

25. Chen B, Zhou D, Zhu L. Transitional adsorption and partition of nonpolar and polar aromatic contaminants by biochars of pine needles with different pyrolytic temperatures. Environ Sci Technol 2008; 42(14): 5137-43.

26. Mimmo T, Panzacchi P, Baratieri M, Davies CA, Tonon G. Effect of pyrolysis temperature on miscanthus (Miscanthus × giganteus) biochar physical, chemical and functional properties. Biomass Bioenergy 2014; 62: 149-57. doi: 10.1016/j.biombioe.2014.01.004.

27. Farasati M, Boroomand Nasab S, Moazed H, Jafarzadeh Haghighifard N, Abedi Koupai J, Seyedian M. Nitrate removal from contaminated waters by using anion exchanger phragmites australis nanoparticles. Water and Wastewater 2013; 24(1): 34-42. [In Persian].

28. Tehrani-Bagha AR, Nikkar H, Mahmoodi NM, Markazi M, Menger FM. The sorption of cationic dyes onto kaolin: Kinetic, isotherm and thermodynamic studies. Desalination 2011; 266(1-3): 274-80. doi: 10.1016/j.desal.2010.08.036.

29. Hameed BH, El-Khaiary MI. Equilibrium, kinetics and mechanism of malachite green adsorption on activated carbon prepared from bamboo by K2CO3 activation and subsequent gasification with CO2. J Hazard Mater 2008; 157(2): 344-51. doi: 10.1016/j.jhazmat.2007.12.105.

30. Fernández-Olmo I, Fernández JL, Irabien A. Purification of dilute hydrofluoric acid by commercial ion exchange resins. Sep Purif Technol 2007; 56(1): 118-25. doi: 10.1016/j.seppur.2007.01.002.